frontiers | Frontiers in Physics

TYPE Original Research
PUBLISHED 15 July 2024
DOI 10.3389/fphy.2024.1410076

OPEN ACCESS

EDITED BY
Chong Qi,
Royal Institute of Technology, Sweden

REVIEWED BY
Priyanka Choudhary,
Royal Institute of Technology, Sweden
Yu Zhang,
Liaoning Normal University, China

*CORRESPONDENCE
Changbo Fu,
cbfu@fudan.edu.cn
Wanbing He,
hewanbing@fudan.edu.cn
Yugang Ma,
mayugang@fudan.edu.cn

RECEIVED 31 March 2024
ACCEPTED 06 June 2024
PUBLISHED 15 July 2024

CITATION
Yang Y, Wang Y, Ma Z, Fu C, He W and Ma Y (2024), Feasibility of probing the NEEC process using storage rings.
Front. Phys. 12:1410076.
doi: 10.3389/fphy.2024.1410076

Feasibility of probing the NEEC process using storage rings

Yi Yang, Yumiao Wang, Zhiguo Ma, Changbo Fu*, Wanbing He* and Yugang Ma*

Key Laboratory of Nuclear Physics and Ion-beam Application (MoE), Institute of Modern Physics, Fudan University, Shanghai, China

One of the fundamental processes in nuclear physics is nuclear excitation by electron capture (NEEC). Having been proposed theoretically for almost 50 years, the experimental confirmation of NEEC is still missing, making it imperative to validate this process. In this paper, we propose a new experimental method based on the anti-coincidence principle to search for the long-anticipated NEEC phenomenon, which involve heavy-ion storage rings. Our calculations indicate that the proposed experimental setup, storage ring, have the potential to surmount background noise, particularly Radiative Recombination (RR) and Coulomb Excitation (CE), and offer a high likelihood of discovering the long-awaited NEEC process.

KEYWORDS

NEEC, storage ring, anti-coincidence, nuclear isomer, nuclear excitation

1 Introduction

The Nuclear Excitation by Electron Capture (NEEC) mechanism involves the capture of an electron to an atomic shell or orbital, which result in the excitation of the atomic nucleus to an excited state [1, 2]. The NEEC process is the reverse process of Internal Conversion (IC), and is regarded as one of the most promising mechanisms for producing isomers for nuclear clocks [3–7], as well as other fields such as medical treatment [8, 9], and nuclear batteries [10–12]. Especially, clocks based on transitions in nuclear energy levels hold the potential for greater accuracy than any existing clock, raising hopes for advancements in timekeeping technology [3, 13–15]. One of promising isotope candidates for nuclear clocks is ^{229m}Th, which has an excited state of around 8.35574 (3) eV [7]. However, a key challenge impeding the realization of a nuclear clock is efficiently exciting a nucleus to its excited state. It is anticipated that NEEC could provide a highly efficient approach to addressing this challenge. By employing a monoenergetic electron beam, the production rate of some isomers can be significantly enhanced, potentially by several orders of magnitude compared to photon beams.

The NEEC process is illustrated in Figure 1. An atom captures a free electron and subsequently transfers the energy, which is the sum of the electron's kinetic energy and the binding energy of the electron to the atomic orbit, to the nucleus. As a result, the nucleus becomes excited from its ground state to an isomeric state.

The first experimental evidence of NEEC about ^{93m}Mo was reported in 2018 [16]. However, subsequent studies by Guo *et al.* [17, 18] expressed reservations. Especially, the theoretical results in Ref. [19] show nine orders of magnitude discrepancy with the experimental excitation probability of 0.010 (3) in Ref. [16]. These works highlighted concerns regarding a potential significant overestimation of the NEEC cross-section in their experimental data analyses. A follow-up experiment conducted by Guo *et al.* [20] in the subsequent year aimed to replicate the studies on ^{93m}Mo, but with significantly reduced

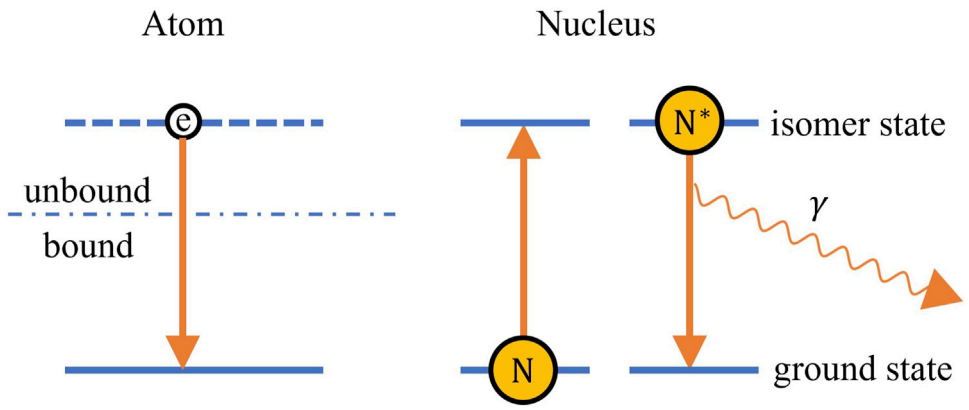

FIGURE 1
The NEEC process illustrated schematically. On the left side is the atomic level of the system, represents the capture of a free electron by a charged ion and transitioning to a bound state. On the right side is the nuclear level, where a nucleus initially in its ground state is excited to an excited state. Subsequently, the nucleus undergoes de-excitation, and then emits a photon.

background noise. This subsequent experiment yielded a negative outcome regarding the excitation of ^{93m}Mo via the NEEC mechanism. Later, J. Rzadkiewicz propose a novel theoretical approach describing the depletion of the ^{93m}Mo isomer, asserting that the Compton profile must be considered in the analysis of the NEEC-RT (NEEC in Resonant Transfer) process [21, 22]. As of now, the exploration of the NEEC process remains ongoing.

In this study, we propose a detection scheme for observing the NEEC process, employing anti-coincidence techniques to suppress background noise, particularly arising from radiative recombination (RR) and Coulomb Excitation (CE) processes. We calculate the NEEC rates for various candidate nuclei. Our results reveal a significant improvement in the signal-to-noise ratio (SNR), thereby underscoring the promise of our proposed scheme.

This paper is structured as follows: Section 1 offers a succinct overview of the historical context of NEEC research. Section 2 presents the theoretical formulas employed for calculating NEEC cross-sections. In Section 3, an alternative approach for validating NEEC using a cooling storage ring will be outlined. A concluding summary will be provided at the end.

2 Theoretical formulas of the cross sections for NEEC

As depicted in Figure 1, the NEEC process involves three states: initial, intermediate, and final states. The initial state can be described as comprising a free electron and a nucleus in its ground state, but no photons present, i.e., $|i\rangle = |\boldsymbol{p}m_s, I_i M_{I_i}, n_{\boldsymbol{k}\sigma} = 0\rangle$. The intermediate state is denoted by $|d\rangle = |nl_j, I_d M_{I_d}, n_{\boldsymbol{k}\sigma} = 0\rangle$, which refers to a state with an electron captured in the orbital of nl_j, a nucleus in its excited state, and no photon involved as well. The final state can be written as $|f\rangle = |nl_j, I_i M_{I_i}, n_{\boldsymbol{k}\sigma} = 1\rangle$, which stands for a state with an electron captured in the orbital of nl_j, an unexcited nucleus, and an emitted photon. $n_{\boldsymbol{k}\sigma}$ is the number of photons with polarization of $\sigma = \pm 1$ and wavenumber and direction of $\boldsymbol{k}$.

According to Fermi's golden rule, the NEEC cross section for a nucleus to capture a free electron with a kinetic energy E_e may be written as [23],

$$\sigma_{NEEC} = \frac{2\pi^2}{p^2}\frac{A_r^{d\to f} Y_n^{i\to d}}{\Gamma_d} L_d(E_e + E_b - \Delta E), \tag{1}$$

where $p^2c^2 = E^2 - m_e^2c^4 = E_e^2 + 2E_e m_e c^2$ denotes the momentum term of a free electron. Since the NEEC is a resonant process, the Lorentz resonance factor is essential [23],

$$L_d(E_e + E_b - \Delta E) = \frac{\Gamma_d/2\pi}{(E_e + E_b - \Delta E)^2 + \frac{1}{4}\Gamma_d^2}, \tag{2}$$

with E_b representing the bound orbital energy of the electron, ΔE for the energy difference between the excitation level and nonexcitation level of a nucleus, and Γ_d for the excitation level width of the nucleus. As the Lorentz profile is normalized to unity, the resonance strength is introduced as,

$$S_{\mathrm{NEEC}} = \frac{2\pi^2}{p^2}\frac{A_r^{d\to f} Y_n^{i\to d}}{\Gamma_d}. \tag{3}$$

As previously indicated, the NEEC process detection consists of two steps, with $Y_n^{i\to d}$ and $A_r^{d\to f}$ representing the reaction rates for excitation and de-excitation, respectively. The formulas of $Y_n^{i\to d}$ and $A_r^{d\to f}$ can also be found in Refs. [23, 24]. Given that the NEEC is inverse to the IC, the excited level width Γ_d in Eqs 1, 2 is determined by,

$$\Gamma_d = A_r^{d\to f} + \frac{2I_d + 1}{2I_i + 1} Y_n, \tag{4}$$

$$A_r = \frac{8\pi(L+1)}{L[(2L+1)!!]^2}\frac{E^{2L+1}}{c} B\downarrow(\lambda L, I_d \to I_f), \tag{5}$$

$$Y_n^{(e)} = \frac{4\pi^2\rho_i}{(2L+1)^2} B\uparrow(EL, I_i \to I_d)(2j_d+1) \times \sum_{\kappa} |R^{(e)}_{L,\kappa_d,\kappa}|^2 C\left(j_d L j; \frac{1}{2}0\frac{1}{2}\right)^2, \tag{6}$$

$$Y_n^{(m)} = \frac{4\pi^2\rho_i}{L^2(2L+1)^2} B\uparrow(ML, I_i \to I_d)(2j_d+1) \times \sum_{\kappa}(2j+1)(\kappa_d+\kappa)^2 \begin{pmatrix} j_d & j & L \\ \frac{1}{2} & \frac{1}{2} & 0 \end{pmatrix}^2 |R^{(m)}_{L,\kappa_d,\kappa}|^2, \tag{7}$$

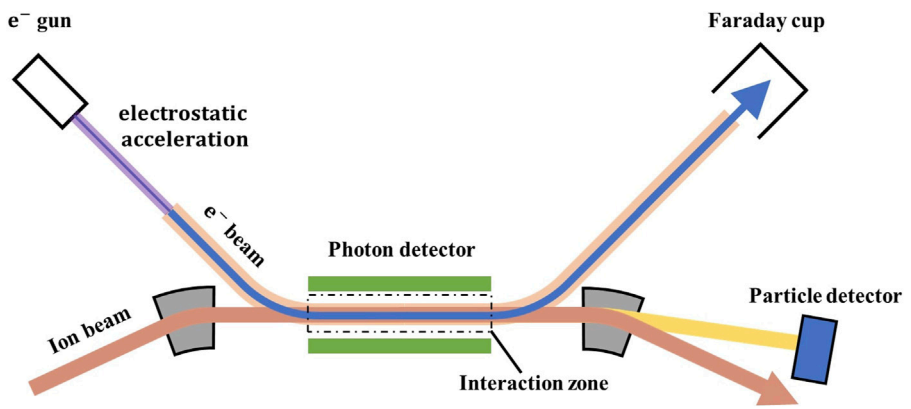

FIGURE 2
Proposed experimental layout for NEEC detection employing a storage ring. The NEEC process takes place in the interaction zone, where the ion beam, circulating in the CSR, interacts with the electron beam. A photon detector array surrounds the interaction zone. Ions excited through NEEC or RR mechanisms are collected by a particle detector. Further details are provided in the main text.

where I_i, I_d and I_f are the spins of the states $|i\rangle$, $|d\rangle$ and $|f\rangle$, B is the reduced transition probability, and ρ_i the density of the initial electronic states, respectively. Other parameters, including j_d, j, and κ, can be studied and extracted from the electron orbital nl_j. The NEEC transition rate Y_n has two different types with $Y_n^{(e)}$ for electric transitions and $Y_n^{(m)}$ for magnetic transitions. The radial integrals involved here can be written as [24],

$$R^{(e)}_{L,\kappa_d,\kappa} = \int_0^\infty dr\ r^{-L+1}\left(f_{n_d\kappa_d}(r)f_{\epsilon\kappa}(r) + g_{n_d\kappa_d}(r)g_{\epsilon\kappa}(r)\right), \quad (8)$$

$$R^{(m)}_{L,\kappa_d,\kappa} = \int_0^\infty dr\ r^{-L+1}\left(g_{n_d\kappa_d}(r)f_{\epsilon\kappa}(r) + f_{n_d\kappa_d}(r)g_{\epsilon\kappa}(r)\right), \quad (9)$$

where $f_{\epsilon\kappa}(r)$ and $g_{\epsilon\kappa}(r)$ in the integrals are parts of the partial-wave expansion of the continuum electronic wave function.

The calculation of NEEC cross sections requires knowledge of the reduced nuclear transition probabilities B $(\lambda L,\ I_i \rightarrow I_d)$ as depicted in Eq. 5. Additionally, the electron's wave function, denoted as $f_{n_d\kappa_d}(r)$ and $g_{n_d\kappa_d}(r)$, is essential for these calculations. In this study, the AMBiT code [25] was employed to compute the electron's wave function; and experimental data for the reduced nuclear transition probabilities B $(\lambda L,\ I_i \rightarrow I_d)$ were utilized.

3 Proposed method for NEEC experiment at storage ring

NEEC shares many characteristics with the resonant process known as dielectronic recombination (DR), in which a free electron is captured and a bound electron is simultaneously excited forming a doubly excited state [26–38]. Instead of a bound electron, the nucleus is excited to a higher level in NEEC. Regarding the detection of NEEC, some researchers have discussed the feasibility on EBIT. In Ref. [39], Jon Ringuette discussed a method of triggering NEEC in ^{129m}Sb at TITAN-EBIT. In Ref. [40], a modified EBIT configuration is described, featuring two electron guns with different energy settings. A. Palffy *et al.* proposed an experimental method for spatially separating photon emissions based on the differing time scales of RR and NEEC process, and provided theoretical evidence that the resonance strength of NEEC could be increased by introduce the fast electronic x-ray decay [41]. In the following, this paper will focus on the discussion of the method applied at storage ring, based on the anti-coincidence principle. And it is expected to benefit the NEEC detection greatly by improving the SNR, as introduced in detail later.

An electron-ion interaction experiment is expected to make the NEEC process observable. And a heavy ion storage ring provides an ideal experimental environment, in which relatively long-lived isomers interact with electron beams, similar to the DR experiment [26, 27, 42].

The proposed setup is shown in Figure 2. The electron beam interacts with the ion beam in the interaction zone, which is surrounded by a photon detector array. A particle detector is located downstream away from the main beam path.

Suppose the ions in the storage ring have charge states of q + and energy of E_i, and the energy of a cooling electron beam is E_e. If the NEEC processes take place, the implicated ion's charge state then changes from q + to $(q-1)$ +, causing the ion to deflect from its normal orbit and hit the particle detector. For NEEC, the nucleus is excited, $A^{*(q-1)+}$, while for RR, the nucleus stays on its ground state, $A^{(q-1)+}$, which normally emit photons immediately at interaction zone, as shown in Figure 3. The main source of noise is that the nucleus $A^{(q-1)+}$ gets excited when it hits the particle detector due to some mechanisms, such as CE. The main idea of the method based on anti-coincidence lies in voting the events in which a photon with energy ΔE is detected in the interaction zone. Because the photon is supposed to come from the RR processes. And in this way, the SNR is expected to be improved.

In the experiment, the NEEC rate is dependent on the relative energy between the electron beam and the ion beam. According to the relativistic velocity formula, the collision energy (E) in the center of mass coordinate (cm) can be written as,

$$E = \gamma\left(E_e - \beta p_e c\right),$$

where $\gamma = \frac{1}{\sqrt{1-\beta^2}}$ and $\beta = v_{cm}/c$, $v_{cm} = c^2\frac{p_e+p_i}{E_e+E_i}$ is the velocity of system, p_e is the momentum of electron, p_i is the momentum of ion, E_e is the energy of the electron in the laboratory coordinate system, and E_i is the energy of

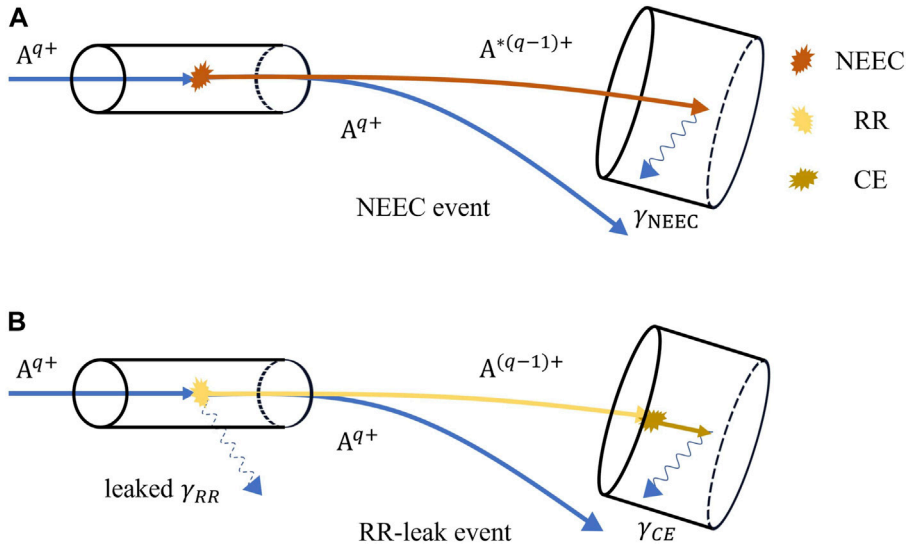

FIGURE 3
Two types of events, **(A)** NEEC events and **(B)** RR-leak events. In NEEC event, the nucleus *A* is on its excited state, i.e., $A^{*(q-1)+}$. For the RR process, the nucleus *A* is on its ground state, i.e., $A^{(q-1)+}$. The events, which are not vetoed by the photon detector array, and also produce CE signals at particle detector, are noted as "RR-leak events". Look the main text for details.

TABLE 1 Reaction rates of NEEC for some candidate isotopes. All isotopes are assumed to be bare nuclei, with electrons captured into their K-shell. The initial state of the nuclei in all cases presented in this table is on their ground states.

HCIs	Life time of isomer (ns)	Transition type	Γ_d (eV)	S_{neec} (b·eV)	ΔE (keV)	E_e (keV)	λ (/s)	SNR
^{61}Ti	200	E2	2.28×10^{-09}	2.37×10^{-4}	125.0	289	3.21×10^{-6}	< 0.1
^{54}V	900	E2	6.43×10^{-10}	7.20×10^{-5}	108.0	265	1.32×10^{-6}	< 0.1
^{74}Ga	31	M1	1.45×10^{-08}	1.99×10^{-3}	56.55	181	1.48×10^{-4}	< 0.1
^{77}Kr	118	E1	3.87×10^{-09}	3.91×10^{-4}	66.50	189	2.03×10^{-5}	21
^{100}Rh	26	E1	1.29×10^{-09}	3.56×10^{-4}	74.78	186	1.43×10^{-5}	30
^{98}Ag	161	E2	2.83×10^{-09}	3.58×10^{-4}	107.2	230	6.66×10^{-6}	< 0.1
^{159}Gd	27.6	E1	1.28×10^{-08}	2.89×10^{-2}	67.83	124	1.43×10^{-3}	17

the ion beam in the laboratory coordinate system. For a given energy distribution function $P(E)$, the reaction rate of NEEC can be expressed as,

$$\lambda_{NEEC} = \int dE \sigma_{NEEC}(E) P(E) \int I_i(\mathbf{r}) n_e(\mathbf{r}) d\mathbf{r}, \qquad (10)$$

with the $I_i(\mathbf{r})$ and $n_e(\mathbf{r})$ representing the ion flux density and the electron density in the interaction zone, respectively.

As examples, some candidates for searching the NEEC process are listed in Table 1. Seven different nuclei are chosen, including ^{61}Ti, ^{54}V, ^{74}Ga, ^{77}Kr, ^{100}Rh, ^{98}Ag, and ^{159}Gd. The parameters used here are listed in Table 2, which are typical experimental conditions for a storage ring. And the NEEC rates for these nuclei are given with Eq. 10, in which the NEEC cross sections are calculated following Eqs 1–9.

The primary source of background noise in NEEC arises from the RR events in the interaction zone, as depicted in Figure 3. To address this challenge, we propose employing an anti-coincidence method to effectively discriminate between NEEC and RR events. Following the bending magnet, ions $A^{*(q-1)+}$ originating from NEEC and $A^{(q-1)+}$ from RR are collected. The occurrence of NEEC is confirmed if photons γ_{NEEC} with energy $E_\gamma = \Delta E$ are detected at the particle detector. Additionally, as illustrated in Figure 2, a photon detector is strategically positioned around the interaction zone to detect RR photons. Taking the anti-coincidence of RR photon signals with the signals from the particle detectors, one will distinguish NEEC events from the RR events, and then have much enhanced SNR,

Figure 3 gives a description of the source of noise, even though we have voted the majority of the RR events. An NEEC event should only be recorded when a photon with energy ΔE is detected at particle detector, but no photon at interaction zone, as shown in Figure 3A. However, an RR-leak event (b) behaves the same because of the limited size and detection efficiency of the veto detector. Obviously, the source of noise happens in the case when RR photon leaks out and the nucleus gets excited at particle detector.

After exiting the storage ring, the isomers were decelerated by the detector materials where they were brought to a complete stop. This stopping process typically takes less than a few nanoseconds. Radiation associated with this period, such as X-rays stemming from atomic processes, bremsstrahlung photons, and most nuclear reaction

TABLE 2 The input parameters utilized for estimating the NEEC rates in the storage-ring scheme.

Parameters	Design metrics
Electron current	1 mA
Electron energy	(depending on E_i and ΔE)
$\Delta E_e/E_e$	10^{-4}
Ion energy	50 MeV/u
$\Delta E_i/E_i$	10^{-4}
Electron beam radius	~ 0.5 mm
Ion beam radius	~ 0.5 mm
Number of Ions in CSRe	10^7
Circumference of CSRe	128 m
Length of cooling section	4 m

products, dissipates at the time when the isomers are totally stopped. Consequently, subsequent detection of isomer decays occurs in an environment free from these backgrounds. Additionally, the gamma-rays emitted from the A^* decay are mono-energetic, facilitating the identification of anticipated events.

Define the SNR to be,

$$SNR \equiv \frac{P_{NEEC}}{P_{RR} * (1-\eta) * P_{CE}},$$

where $P_{NEEC}(P_{RR})$ is the possibility of the NEEC (RR) process in the interaction zone, P_{CE} is for CE process in the particle detector and $\eta > 99\%$ is the detecting efficiency of photons. Taking ^{159}Gd as an example, $P_{NEEC} = 2.5 \times 10^{-6}$ and $P_{RR} = 1 - P_{NEEC} \sim 1$, and $P_{CE} < 1.4 \times 10^{-5}$. Taking these values, an SNR of higher than 17 is expected. Noting that the RR cross section utilized in the calculation is supported by the FAC (Flexible Atomic Code) program [43], and the CE cross section is computed using the method outlined in Ref. [44], as described in Equations II B. (37) – (38).

Several heavy ion storage rings can be used for this proposed experiment. For example, there are storage rings at the IMP in Lanzhou, China [45–47]. The facility has a main cooler storage ring (CSRm) as a synchrotron, an experimental cooler storage ring (CSRe), a radioactive beam line as fragment separator (RIBLL2), and several experimental terminals. The heavy ions with energy of several MeV u^{-1} delivered from the cyclotron are first injected into the CSRm, cooled, and accelerated to several hundred MeV u^{-1} in the CSRm. Then the ions are extracted and delivered to the CSRe. Isotopes with a relatively short life time, which may benefit NEEC studies, can be generated and stored in the ring. As an illustration, ^{74}Ga can be produced with reaction ^{76}Ge$(p,^3$He$)^{74}$Ga and then sent to CSRe with an intensity of $> 10^8$. A simulation, with the experimental assumption listed in Table 2, demonstrates that the proposed setup allows for the observation of NEEC events with rate of tens of events per day by taking the isomer decay in the flight before being stopped in the particle detector.

It should be noted that a significant δE can potentially disrupt the stability of ions within a CSR, consequently limiting the number of orbits an ion can maintain within the CSR. The contradiction created by the dual uses of electron beam energy to sustain the ion beam and induce NEEC may have two potential solutions: either select a reaction system whose resonance energy is within the range to maintain the ion beam, or optimize the experimental setup. HIAF [48] may offer a workable solution: build two electron beams, one for cooling electrons to preserve beam stability and the other for resonance electrons, which can be applied to DR as well as NEEC experiments.

4 Summary

In this manuscript, we propose an anti-coincidence approach for NEEC studies employing storage rings. Simulations of NEEC rates for different candidate nuclei are conducted. With the adoption of parameters deemed practically acceptable, our simulations demonstrate that a high signal-to-noise ratio of approximately five can be achieved for certain nuclei such as ^{77}Kr, ^{100}Rh and ^{159}Gd, as detailed in Table 1. The execution of these suggested experiments holds the potential to validate the presence of NEEC. Such advancements would have far-reaching implications across various domains, including nuclear astrophysics, nuclear clocks, nuclear medicine, and beyond.

Data availability statement

The original contributions presented in the study are included in the article, further inquiries can be directed to the corresponding authors.

Author contributions

YY: Conceptualization, Data curation, Formal Analysis, Investigation, Methodology, Software, Validation, Visualization, Writing–original draft, Writing–review and editing. YW: Data curation, Formal Analysis, Validation, Writing–review and editing. ZM: Investigation, Validation, Visualization, Writing–review and editing. CF: Conceptualization, Funding acquisition, Investigation, Methodology, Project administration, Resources, Supervision, Writing–original draft, Writing–review and editing. WH: Conceptualization, Project administration, Resources, Software, Supervision, Writing–original draft, Writing–review and editing. YM: Funding acquisition, Project administration, Resources, Supervision, Writing–original draft, Writing–review and editing.

Funding

The author(s) declare that financial support was received for the research, authorship, and/or publication of this article. This work is supported by the National Key R&D Program of China (No. 2023YFA1606900, 2022YFA1602402, 2020YFE0202001) and the National Natural Science Foundation of China (NSFC) under Grant (No. 12235003).

Conflict of interest

The authors declare that the research was conducted in the absence of any commercial or financial relationships that could be construed as a potential conflict of interest.

Publisher's note

References

1. Goldanskii V, Namiot V. On the excitation of isomeric nuclear levels by laser radiation through inverse internal electron conversion. *Phys Lett B* (1976) 62:393–4. ISSN 0370-2693. doi:10.1016/0370-2693(76)90665-1

2. Palffy A. Nuclear effects in atomic transitions. *Contemp Phys* (2010) 51:471–96. ISSN 0010-7514. doi:10.1080/00107514.2010.493325

3. Beeks K, Sikorsky T, Schumm T, Thielking J, Okhapkin MV, Peik E. The thorium-229 low-energy isomer and the nuclear clock. *Nat Rev Phys* (2021) 3:238–48. doi:10.1038/s42254-021-00286-6

4. von der Wense L, Seiferle B. The ^{229}Th isomer: prospects for a nuclear optical clock. *Eur Phys J A* (2020) 56:277. ISSN 1434-601X. doi:10.1140/epja/s10050-020-00263-0

5. Wang W, Zhou J, Liu B, Wang X. Exciting the isomeric Th229 nuclear state via laser-driven electron recollision. *Phys Rev Lett* (2021) 127:052501. doi:10.1103/PhysRevLett.127.052501

6. Qi J, Zhang H, Wang X. Isomeric excitation of Th229 in laser-heated clusters. *Phys Rev Lett* (2023) 130:112501. doi:10.1103/PhysRevLett.130.112501

7. Tiedau J, Okhapkin MV, Zhang K, Thielking J, Zitzer G, Peik E, et al. Laser excitation of the Th-229 nucleus. *Phys Rev Lett* (2024) 132:182501. doi:10.1103/PhysRevLett.132.182501

8. Surti S, Pantel AR, Karp JS. IEEE transactions on radiation and plasma medical sciences. *IEEE Trans Radiat Plasma Med Sci* (2020) 4:283–92. ISSN 2469-7311. doi:10.1109/trpms.2020.2985403

9. Lan H-Y, Wu D, Liu J-X, Zhang J-Y, Lu H-G, Lv J-F, et al. Photonuclear production of nuclear isomers using bremsstrahlung induced by laser-wakefield electrons. *Nucl Sci Tech* (2023) 34:74. ISSN 1001-8042. doi:10.1007/s41365-023-01219-x

10. Kirischuk V, Ageev V, Dovbnya A, Kandybei S, Ranyuk Y. Induced acceleration of the decay of the 31-yr isomer of 178m^2 Hf using bremsstrahlung radiation. *Phys Lett B* (2015) 750:89–94. doi:10.1016/j.physletb.2015.08.051

11. Karpeshin FF, Trzhaskovskaya MB, Vitushkin LF. Electron recombination as a way of deexciting the 129mSb isomer. *Bull Russ Acad Sci Phys* (2020) 84:1207–9. ISSN 1934-9432. doi:10.3103/S1062873820100135

12. Rzadkiewicz J, Polasik M, Slabkowska K, Syrocki L, Weder E, Carroll JJ, et al. Beam-based scenario for Am242m isomer depletion via nuclear excitation by electron capture. *Phy Rev C* (2019) 99:044309. ISSN 2469-9985. doi:10.1103/physrevc.99.044309

13. Soff G, de Reus T, Müller U, Reinhardt J, Müller B, Greiner W. *Atomic clock phenomena in collisions of very heavy ions*. Boston, MA: Springer US (1987). p. 81–110. ISBN 978-1-4613-1889-7. doi:10.1007/978-1-4613-1889-7_5

14. Campbell CJ, Radnaev AG, Kuzmich A, Dzuba VA, Flambaum VV, Derevianko A. Single-ion nuclear clock for metrology at the 19th decimal place. *Phys Rev Lett* (2012) 108:120802. ISSN 0031-9007. doi:10.1103/physrevlett.108.120802

15. Peik E, Tamm C. Nuclear laser spectroscopy of the 3.5 eV transition in Th-229. *Europhys Lett* (2003) 61:181–6. ISSN 0295-5075. doi:10.1209/epl/i2003-00210-x

16. Chiara CJ, Carroll JJ, Carpenter MP, Greene JP, Hartley DJ, Janssens RVF, et al. *Nature* (2018) 554:216+. doi:10.1038/nature25483

17. Guo S, Fang Y, Zhou X, Petrache CM. Possible overestimation of isomer depletion due to contamination. *Nature* (2021) 594:E1–2. ISSN 0028-0836. doi:10.1038/s41586-021-03333-5

18. Chiara CJ, Carroll JJ, Carpenter MP, Greene JP, Hartley DJ, Janssens RVF, et al. Reply to: possible overestimation of isomer depletion due to contamination. *Nature* (2021) 594:E3–4. ISSN 0028-0836. doi:10.1038/s41586-021-03334-4

19. Wu Y, Keitel CH, Palffy A. Solving statistical mechanics using variational autoregressive networks. *Phys Rev Lett* (2019) 122:080602. ISSN 0031-9007. doi:10.1103/physrevlett.122.080602

20. Guo S, Ding B, Zhou XH, Wu YB, Wang JG, Xu SW, et al. Probing Mo93m isomer depletion with an isomer beam. *Phys Rev Lett* (2022) 128:242502. doi:10.1103/PhysRevLett.128.242502

21. Rzadkiewicz J, Polasik M, Slabkowska K, Syrocki L, Carroll JJ, Chiara CJ. Novel approach to Mo93m isomer depletion: nuclear excitation by electron capture in resonant transfer process. *Phys Rev Lett* (2021) 127:042501. ISSN 0031-9007. doi:10.1103/physrevlett.127.042501

22. Rzadkiewicz J, Słabkowska K, Polasik M, Syrocki L, Carroll JJ, Chiara CJ. Mo93m isomer depletion via nuclear excitation by electron capture in resonant transfer into highly excited open-shell atomic states. *Phys Rev C* (2023) 108:L031302. doi:10.1103/PhysRevC.108.L031302

23. Palffy A, Scheid W, Harman Z. Theory of nuclear excitation by electron capture for heavy ions. *Phys Rev A* (2006) 73:012715. ISSN 1050-2947. doi:10.1103/physreva.73.012715

24. Gagyi-Palffy A. *Theory of nuclear excitation by electron capture for heavy ions* [Ph.D. thesis]. Justus Liebig University Giessen, Giessen, Germany (2006). Available from: https://core.ac.uk/display/56343138?utm_source=pdf&utm_medium=banner&utm_campaign=pdf-decoration-v1.

25. Emily K, Julian B. *Ambit 3.1* (2023). Available from: https://github.com/jturney/ambit (Accessed July 2024).

26. Yao K, Geng Z, Xiao J, Yang Y, Chen C, Fu Y, et al. KLL dielectronic recombination resonant strengths of He-like up to O-like xenon ions. *Phys Rev A* (2010) 81:022714. doi:10.1103/PhysRevA.81.022714

27. Hu Z, Xiong G, He Z, Yang Z, Numadate N, Huang C, et al. Giant retardation effect in electron-electron interaction. *Phys Rev A* (2022) 105:L030801. doi:10.1103/PhysRevA.105.L030801

28. Xu T, Xiong G, Xiao J, Yang Y, Hutton R, Zou Y, et al. K-shell excitation dielectronic recombination resonance strengths of highly charged He-like to O-like Xe ions. *Plasma Sci Technol* (2018) 20:074010. ISSN 1009-0630. doi:10.1088/2058-6272/aac573

29. Huang ZK, Wen WQ, Wang SX, Khan N, Wang HB, Chen CY, et al. Absolute rate coefficients for dielectronic recombination of Na-like Kr25+. *Phys Rev A* (2020) 102:062823. ISSN 2469-9926. doi:10.1103/physreva.102.062823

30. Wen W, Huang Z, Wang S, Khan N, Wang H, Chen C, et al. Rate coefficients for dielectronic recombination of carbon-like $^{40}Ca^{14+}$. *Astrophysical J* (2020) 905:36. doi:10.3847/1538-4357/abc1e4

31. DeWitt DR, Schneider D, Chen MH, Clark MW, McDonald JW, Schneider MB. Dielectronic recombination cross sections of neonlike xenon. *Phys Rev Lett* (1992) 68:1694–7. doi:10.1103/PhysRevLett.68.1694

32. Brandau C, Kozhuharov C, Müller A, Shi W, Schippers S, Bartsch T, et al. Precise determination of the2s1/2–2p1/2Splitting in very heavy lithiumlike ions utilizing dielectronic recombination. *Phys Rev Lett* (2003) 91:073202. doi:10.1103/PhysRevLett.91.073202

33. Ralchenko Y, Gillaspy JD. Anisotropic LMN dielectronic resonances from ratios of magnetic-dipole lines. *Phys Rev A* (2013) 88:012506. doi:10.1103/PhysRevA.88.012506

34. Kilgus G, Berger J, Blatt P, Grieser M, Habs D, Hochadel B, et al. Dielectronic recombination of hydrogenlike oxygen in a heavy-ion storage ring. *Phys Rev Lett* (1990) 64:737–40. doi:10.1103/PhysRevLett.64.737

35. Watanabe H, Tobiyama H, Kavanagh AP, Li YM, Nakamura N, Sakaue HA, et al. Dielectronic recombination of He-like to C-like iodine ions. *Phys Rev A* (2007) 75:012702. doi:10.1103/PhysRevA.75.012702

36. Mohamed T, Nikolić D, Lindroth E, Madzunkov S, Fogle M, Tokman M, et al. Dielectronic recombination of lithiumlike beryllium: a theoretical and experimental investigation. *Phys Rev A* (2002) 66:022719. doi:10.1103/PhysRevA.66.022719

37. Fuchs T, Biedermann C, Radtke R, Behar E, Doron R. Channel-specific dielectronic recombination of highly charged krypton. *Phys Rev A* (1998) 58:4518–25. doi:10.1103/PhysRevA.58.4518

38. Ali R, Bhalla CP, Cocke CL, Stockli M. Dielectronic recombination on heliumlike argon. *Phys Rev Lett* (1990) 64:633–6. doi:10.1103/PhysRevLett.64.633

39. Ringuette J. *Towards Nuclear Excitation via Electron Capture in an Electron Beam Ion Trap* [Ph.D. thesis]. Colorado School of Mines, Golden, CO, United States (2022). Available from: https://www.proquest.com/dissertations-theses/towards-nuclear-excitation-via-electron-capture/docview/2740532133/se-2.

40. Wang Y, Ma Z, Yang Y, Fu C, He W, Ma Y. Feasibility study of nuclear excitation by electron capture using an electron beam ion trap. *Front Phys* (2023) 11. doi:10.3389/fphy.2023.1203401

41. Palffy A, Harman Z, Kozhuharov C, Brandau C, Keitel CH, Scheid W, et al. Nuclear excitation by electron capture followed by fast x-ray emission. *Phys Lett B* (2008) 661:330–4. ISSN 0370-2693. doi:10.1016/j.physletb.2008.02.027

42. Huang Z, Wang S, Wen W, Wang H, Ma W, Chen C, et al. Absolute dielectronic recombination rate coefficients of highly charged ions at the storage ring CSRm and CSRe. *Chin Phys B* (2023) 32:073401. ISSN 1674-1056. doi:10.1088/1674-1056/acbc69

43. Gu MF. *Flexible-atomic-code* (2023). Available from: https://github.com/flexible-atomic-code/fac (Accessed July 2024).

44. Alder K, Bohr A, Huus T, Mottelson B, Winther A. Study of nuclear structure by electromagnetic excitation with accelerated ions. *Rev Mod Phys* (1956) 28:432–542. doi:10.1103/RevModPhys.28.432

45. Xia J, Zhan W, Wei B, Yuan Y, Song M, Zhang W, et al. The heavy ion cooler-storage-ring project (HIRFL-CSR) at Lanzhou. *Nucl Instrum Methods Phys Res Sect A* (2002) 488:11–25. doi:10.1016/s0168-9002(02)00475-8

46. Wang G-H, Jiang B-C, Tan J-H, Zhang Q-L, Fang W-C, Li C-L, et al. Study on crab-cavity-based longitudinal injection scheme and prototype realization of C-band crab cavity for electron storage rings. *Nucl Sci Tech* (2023) 34:102. ISSN 1001-8042. doi:10.1007/s41365-023-01257-5

47. Liu L-K, Pei H, Wang Y-P, Zhang B, Xu N, Shi S-S. Event plane determination from the zero degree calorimeter at the cooling storage ring external-target experiment. *Nucl Sci Tech* (2023) 34:100. ISSN 1001-8042. doi:10.1007/s41365-023-01262-8

48. Zhou X, Yang Jthe HIAF Project Team. Status of the high-intensity heavy-ion accelerator facility in China. *AAPPS Bull* (2022) 32:35. ISSN 2309-4710. doi:10.1007/s43673-022-00064-1